Journal of Materials Chemistry A

Bridged and Fused Triazolic Energetic Frameworks with an Azo Building Block towards Thermally Stable and Applicable Propellant Ingredients

Journal:	*Journal of Materials Chemistry A*
Manuscript ID	TA-ART-09-2021-007520.R1
Article Type:	Paper
Date Submitted by the Author:	09-Oct-2021
Complete List of Authors:	Shreeve, Jean'ne; University of Idaho, Chemistry Yu, Qiong; University of Idaho, Chemistry Li, Fengsheng ; Beijing Institute of Technology, School of Materials Science and Engineering Yin, Ping; Beijing Institute of Technology, Materials Science and Engineering Pang, Si-Ping; Beijing Institute of Technolodgy, Staples, Richard; Michigan State University, Chemistry

ARTICLE

Bridged and Fused Triazolic Energetic Frameworks with an Azo Building Block towards Thermally Stable and Applicable Propellant Ingredients

Received 00th January 20xx,
Accepted 00th January 20xx

DOI: 10.1039/x0xx00000x

Qiong Yu,[⊥a] Fengsheng Li,[⊥b] Ping Yin,*[b] Siping Pang,*[b] Richard J. Staples,[c] Jean'ne M. Shreeve*[a]

The assembly of nitrogen-rich building blocks determines the energy storage capacity and affects the stability of energetic materials. Owing to the environmentally harmful properties of the propellant, ammonium perchlorate (AP), much research has explored halogen-free replacements which often suffer from poor thermal stability. In our goal of balancing performance and stability, we report access to an energetic molecule (**3**) by smart assembly of an azo bridge into trinitromethyl triazoles. Compound **3** exhibits a decomposition temperature of 175 °C, which approaches the highest among reported trinitromethyl derivatives. The density (1.91 g cm^{-3}) and oxygen balance (+29%) for **3** exceed other candidates, suggesting it as a high energy dense oxidizer (HEDO) replacement for AP in rocket propellants. One-step azo-involved cyclization of **3** give two fused nitro triazolones, (FNTO) **4** and its *N*-oxide **5**, having thermal stabilities and energies superior to the analogous derivatives of 5-nitro-2,4-dihydro-3*H*-1,2,4-triaole-3-one (NTO). The comparison of properties of the fused triazolones **4** and **8** and their *N*-oxide derivatives **5** and **9** shows that formation of an *N*-oxide is an effective strategy which results in an increase of the decomposition temperature, oxygen balance, specific impulse, and detonation properties and in a decrease of the sensitivity of the corresponding energetic material. This work highlights bridged and fused triazolic energetic frameworks with an azo building block providing an alternative structural motif for seeking an applicable high-energy ingredient.

Introduction

Since Alfred Nobel successfully stabilized nitroglycerine by smart composite formulation a century and a half ago, sustained research efforts have been focused on high-energy density materials (HEDMs) by the scientific community. Although high energy and good stability are the continuing criteria for energetic materials, frontier research tends to stabilize these meta-stable ingredients from the molecular level. The rapid development of high-energy compounds provides a multi-disciplinary platform by merging not only composite materials, but also molecular design and synthetic innovation. Searching for new applicable HEDMs to replace the current benchmark materials is an effective way to improve the energy level.[1-3] However, the generation of new energetic molecules has faced a long-term scientific challenge since the pursuit of high-energy is at variance with safety requirements in production, storage, and transportation.

In general, synthetic innovation focused on rationalized energetic functionalization and new molecular scaffolds are the primary pathways to access new HEDMs. Therefore, most investigations have been devoted to the construction of nitrogen-rich heterocycles, as well as the smart late-stage functionalization of these high-energy backbones. Based on the structural features of high-energy molecules, rational incorporation of various nitrogen-rich building blocks is one of the most vital factors used to balance the energetic performance and stability. As one of the most important branches of HEDMs, the propellant is widely applied as the main power source in the design of rockets, missiles and launch vehicles. The major objective in the development of solid rocket propellants is to increase the energy. Currently, ammonium perchlorate (AP) which has been used as an excellent oxidizer in solid rocket propellants for many decades.[4] However, it releases perchlorate into groundwater systems and generates hydrogen chloride during burning likely resulting in environmental problems such as enhancing acid rain and depletion of the ozone layer.[5] Some promising AP replacements, e.g. ammonium dinitramide (ADN)[6] and hydrazinium nitroformate (HNF) [7] have been developed, but their overall energetic properties are still not competitive with AP.[8,9]

In the pursuit of next generation high energy dense oxidizers (HEDOs), the consensus strategy has been established that heterocyclic nitrogen-rich oxidizers could be potential candidates for eco-friendly and stable HEDOs.[10] The extensive recent progress of azole-based oxidizers gives rise to a renaissance in the synthetic innovation of new HEDOs (Fig. 1a,

[a] *Department of Chemistry, University of Idaho, Moscow, ID 83844-2343, United States.*
[b] *School of Materials Science & Engineering, Beijing Institute of Technology, Beijing 100081.*
[c] *Department of Chemistry, Michigan State University East Lansing, MI, 48824, (USA).*
[⊥] These authors contributed equally.
Electronic Supplementary Information (ESI) available: Experimental details for the preparation, theoretical calculations, characterization of materials (PDF). See DOI: 10.1039/x0xx00000x

a-**i**).[11-17] Among them, compound **a** has the best thermal stability of 164 °C; unfortunately, the oxygen balance (9%) is not satisfactory.[11] Compound **i** has the best oxygen balance of 32%

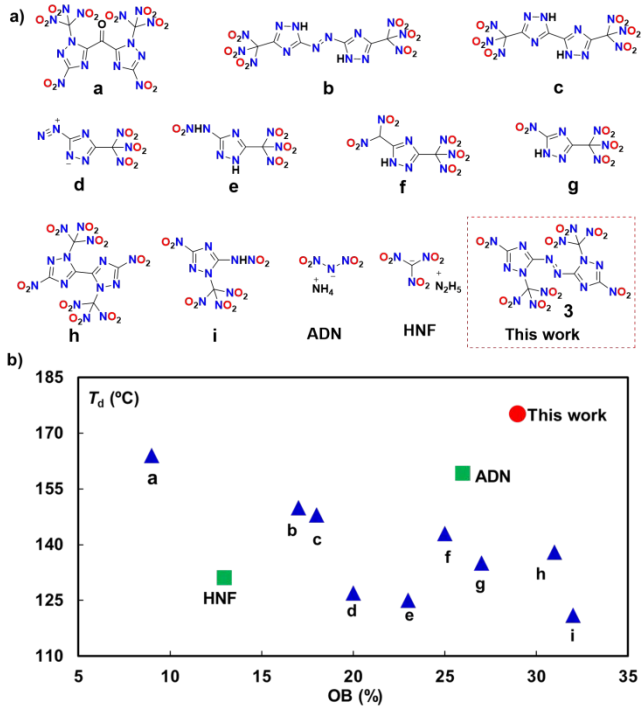

Fig. 1 (a) Structures of ammonium dinitramide (ADN) and hydrazinium nitroformate (HNF), and selected molecules (**a**-**i**, and **3**) containing the trinitromethyl functionality.[11-17] (b) Comparison of decomposition temperatures and oxygen balances of oxidizers.

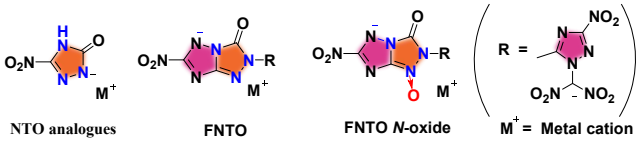

Scheme 1 NTO, FNTO, and FNTO *N*-oxide as propellant ingredients.

but a decomposition temperature of 121 °C limits its application.[13]

With the continuing goal of seeking new propellant ingredients, a bridged triazolic molecule (Fig. 1a, **3**) was designed and synthesized by virtue of introducing an azo functionality. In comparison with previously explored HEDOs, **3** not only has a high density of 1.91 g cm^{-3}, but also competes well between thermal stability and oxygen balance (Fig. 1b). Furthermore, the azo link could be a key building block in the one-step construction of the fused nitrotriazolone (FNTO) and its *N*-oxide (Scheme 1). Compared to the well- known analogues, the metal salts of 5-nitro-2,4-dihydro-3*H*-1,2,4-triaole-3-one (NTO), **FNTO** and its *N*-oxide show remarkably enhanced thermal stability, which highlights its potential application for modifying burning rates in the combustion of solid propellants.[18] Hence, the fused triazolic framework FTNO from the azo precursor may provide an alternative structural motif for seeking a high-energy ingredient.

Results and discussion

Synthesis

N-alkyl-functionalized 3-amino-5-nitro-1,2,4-triazole (**1**)[19] was synthesized based on a literature method, in which 5-amino-3-nitro-1,2,4-triazole (ANTA)[20] reacted with bromoacetone under alkaline conditions (yield, 90%). Initially, **1** was treated with potassium permanganate in conc. HCl which gave the azo bridged product **2** in a yield of 92% (Scheme 2). The reaction with potassium permanganate required 72 hours. To shorten the reaction time, tert-butyl hypochlorite was used as an azo-coupling reagent which gave the bistriazole compound **2** in 5 hours in a yield of 69%. Compound **2** was nitrated by using a mixture of 90% HNO_3 and 98% H_2SO_4 to yield the octanitroazotriazole **3** (81%) which was at 0 °C for 2 h followed by warming to r. t. for another 72 h. Based on the reductants of the trinitromethyl group used in the previous literature, potassium iodide and hydroxylamine in alkaline medium were chosen to explore new dinitromethyl derivatives.[21] Using potassium iodide as the reducing reagent, intramolecular cyclization of **3** gave rise to the fused triazole-triazolone **4** in 84% yield. When hydroxylammonium hydrochloride was chosen as the reagent in the presence of potassium hydroxide, fused triazole-triazolone **5**, the *N*-oxide analogue of **4**, was obtained with good reaction selectivity. Compounds **3**-**5** are stable at room temperature.

Inspired by novel fused structures and promising *N*-oxide functionality, continuing synthesis work was employed to explore energetic molecular and ionic derivatives from **4** and **5** (Scheme 3). It is worthwhile to note that the neutralization of **4** only resulted in the unstable molecule **6**, which must be stored

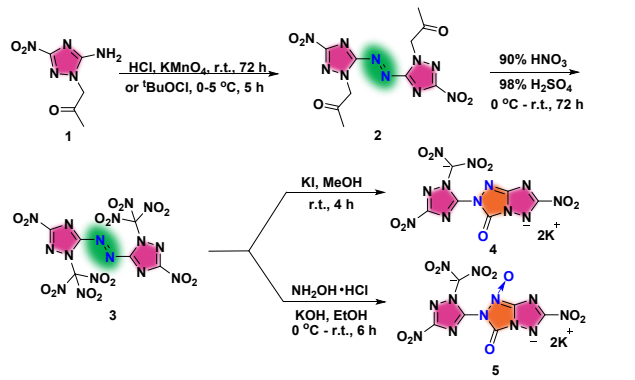

Scheme 2 Synthesis of octanitroazotriazole (**3**), fused triazolone (**4**) and its *N*-oxide (**5**).

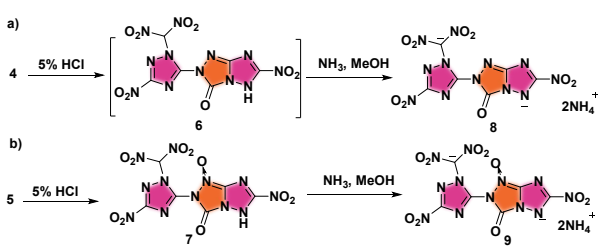

Scheme 3 Energetic molecular and ionic derivatives from **4** and **5**.

in ether solution and was further stabilized as an ionic derivative **8** using ammonia. In comparison, *N*-oxide analogue **7** can be isolated in a neat form and stored for an extended period. Under identical ionization, **9** was formed in good yield. Other bases, e.g. hydrazine and hydroxylamine were tried in order to prepare additional ionic derivatives; however, purification and characterization were hampered by their extreme air sensitivity.

Characterization

All newly synthesized compounds are fully characterized by multinuclear NMR and infrared spectroscopy, differential scanning calorimetry, and elemental analyses. More detailed structural information was acquired by single crystal X-ray diffraction analyses for **3-5**. Their crystallographic data and data collection parameters, bond lengths, and bond angles are in the Electronic Supplementary Information (ESI). Compound **3** crystallizes from dichloromethane in the orthorhombic space group $Pca2_1$ with an excellent crystal density of 1.966 g·cm^{-3} at 100 K. As shown in Fig. 2a, the two triazole rings together with the C2-nitro, C4-nitro and N(1)-N(2) atoms are approximately in the same plane, which plays an important role in the high density of **3**. Specifically, the dihedral angle between the mean planes through the two triazole rings is 8.15°. In addition, the dihedral angle between the mean planes of triazole and corresponding nitro groups is 7.474° [N(3)-N(4)-C(2)-N(5)-C(1) and O(1)-N(9)-O(2)] and 2.599° [N(6)-N(7)-C(4)-N(8)-C(3) and O(3)-N(10)-O(4)]. In contrast, the trinitromethyl moieties are nearly perpendicular to the triazole plane with the dihedral angle between the mean plane through the triazole rings and mean plane through three nitrogen atoms of the $C(NO_2)_3$ moieties lying in the range of 83.2° to 85.7°. The C-NO_2 bond lengths, involving nitro groups directly bonded to the triazole rings [C(2)-N(9) = 1.461 and C(4)-N(10) = 1.463 Å] are significantly shorter relative to the C-NO_2 bond lengths of the $C(NO_2)_3$ moiety [1.538 to 1.556 Å]. This clearly supports the high energy content and lower stability imported by the $C(NO_2)_3$ moiety compared to the nitro groups directly bonded to the triazole ring.

Compound **4** crystallizes by slow evaporation at room temperature from water in the monoclinic space group $P2_1/n$ with four molecules per unit cell, and a density of 2.070 g cm^{-3} at 271 K. Interestingly, as is seen in Fig. 2b and 2c, there are two different forms of existence in the single-crystal X-ray structure of **4** due to constraint of the rigid C(2)-N(7) bond. The structure observed in the Fig. 2b is the major conformation (75%) in the single-crystal X-ray structure (**4a**), whereas the structure in Fig. 2c is the minor form (**4b**, 25%) because of steric hindrance between the O7 atom and the *gem*-dinitromethyl group. The two forms of **4** were also observed in its ^{13}C NMR spectrum which has eleven resonances. All atoms of the *gem*-dinitromethyl group are almost coplanar, whereas the dihedral angle between the gem-dinitromethyl group and the vicinal triazole ring is 76.06°. In addition, the dihedral angle between the mean planes of triazole and fused heterocyclic ring is 33.06° (ESI).

Analogous to the potassium salt **4**, compound **5** crystallizes from water by slow evaporation at room temperature in the monoclinic space group $P2_1/n$ with four molecules per unit cell (Fig. 2d). The structural features are almost the same as that of **4;** however, **5** has one additional coordinated oxygen than **4** that contributes to a higher density (2.131 g cm^{-3} at 296 K). The torsion angle between the *gem*-dinitromethyl group and its bonded triazole ring is 76.30°, whereas the dihedral angle between two neighboring triazoles is 33.08°.

The intermolecular interactions of crystal **3** were studied by the associated Hirshfeld surface and two-dimensional (2D)-fingerprints.[22] As shown in Fig. 3 (a), the blue and red regions on the Hirshfeld surfaces represent low and high close contact populations, respectively. There are some red dots located on the surface edges viewed from the a, b, and c directions, respectively, which indicate strong inter and intramolecular O···O interactions. These interactions have the highest ratios among all kinds of interactions (58.7%) (Fig. 3c). It is because the two trinitromethyl moieties of crystal **3** display a molecular geometry with a propeller-type orientation, which increases the chances to form the O···O interactions. Therefore, **3** has a higher density and is more sensitive towards impact and friction than molecules having fewer nitro groups. The strong intermolecular (N···O and O···N) interactions are shown in crystal **3**, which were

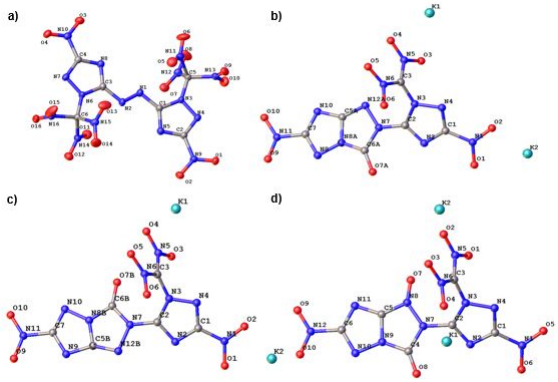

Fig. 2 (a) Single-crystal X-ray structure of **3**. (b) The main form of existence (75%) in the single-crystal X-ray structure of **4a**. (c) The secondary form of existence (25%) in the single-crystal X-ray structure of **4b**. (d) Single-crystal X-ray structure of **5**.

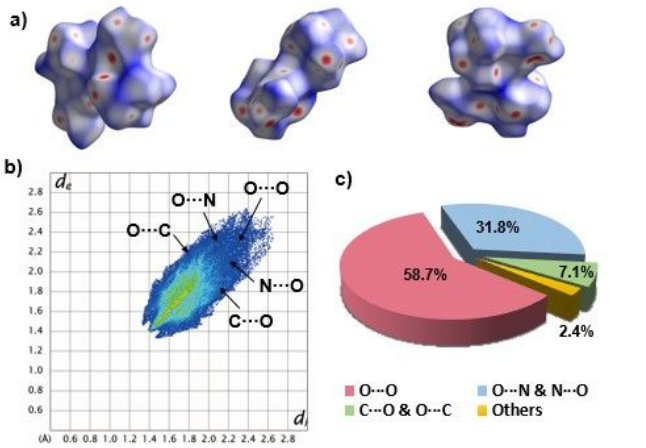

Fig. 3 (a) Hirschfeld surface of crystal **3**. (b) 2D fingerprint plot of crystal **3**. (c) The percentage contribution of individual atomic contacts to the Hirshfeld surface for crystal **3**.

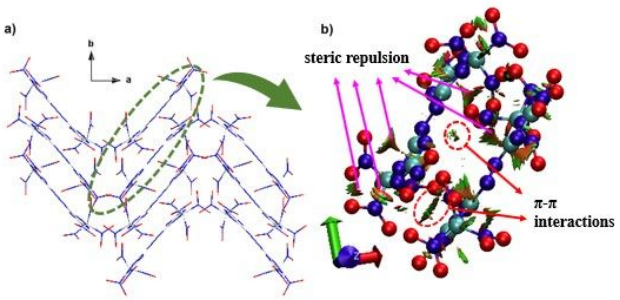

Fig. 4 (a) Packing diagram of **3** viewed along the *c* axis. (b) Noncovalent interaction analysis, including hydrogen bonds and π-π interactions for crystal **3**; the structures were extracted from the packing diagram (green oval in Fig. 4a).

specified on top of the fingerprint plot. There are no hydrogen bonds in the crystal of **3**, and as a result, no spike is observed in Fig. 3(b). Block-shaped surfaces contribute more efficiently to face-to-face π-π stacking, which often are seen as C···O interactions.[23] The ratio of C···O and O···C interactions in crystal **3** (7.1%) indicates face-to-face π-π stacking in **3**, which contributes to the high density and thermal stability of **3**.

The face-to-face π-π stacking is easily observed from the packing diagram of **3** (Fig. 4a), which shows a wave arrangement. Each molecule is parallel to each other except for the *gem*-trinitromethyl groups. The structures extracted from the packing diagram (green oval in Fig. 4a) were analysed by noncovalent interaction analysis (NIC), which can better illustrate the effects of intra- and intermolecular interactions and the azo linkage on crystal packing. The NIC is an invaluable approach to identify noncovalent interactions based on the analysis of electron density and the reduced density gradient,[24] in which the geometry of **3** was optimized using the ORCA 3.0 program[25], and the noncovalent interactions plot was calculated and visualized by Multiwfn[26] and the VMD program,[27] respectively. As shown in Fig. 4b, the red isosurfaces located around the trinitromethyl moieties denote steric repulsion, which result in the high sensitivity. In addition, there are no blue isosurfaces on the edge, indicating that the dimeric stabilization is dominated by face-to-face π-π stacking interactions, which is in agreement with the result of the 2D fingerprint spectra. Furthermore, it is suggested that the system of azo bridged triazoles contributed to form face-to-face π-π stacking interactions in which isosurfaces for face-to-face π-π stacking are observed around the azo linkage and triazole rings. The interactions of face-to-face π-π stacking are expected to give high thermal stability to **3**.

Physical and Detonation Properties

These new molecules and ionic compounds have moderate to excellent thermal stability as determined by differential scanning calorimetric (DSC) measurements. The decomposition temperature of **3** is 175 °C (Table 1), which to our knowledge is the highest among all reported gem-trinitromenthyl functionality compounds. The potassium salts of fused triazolone **4** and *N*-oxide fused triazolone **5** also have good thermal stabilities of 277 and 292 °C, respectively. Interestingly, the ammonium salts of the fused triazolone (**8**) and *N*-oxide fused triazolone (**9**) exhibit the same trends as **4** and **5**, whose decompostion temperatures are 175 and 202 °C, respectively. Compound **7** has the lowest thermal stability decomposing at 129 °C which arises from the presence of the *N*-dinitromethyl group. The densities of **3**-**5** and **7**-**9** were measured by using a gas pycnometer at 25 °C, and lie in the range of 1.78-2.13 g cm^{-3}. It is worthwhile to note that the fused triazolone *N*-oxide **5** has a high density (2.131 g cm^{-3}) outperforming its analogue **4** (2.070 g cm^{-3}) as well as the potassium salt of NTO (**K-NTO**, 1.892 g cm^{-3}). Also, benefiting from azo or fused rings, most compounds exhibit favorable calculated heats of formation, which were computed by using the method of isodesmic reactions (Scheme S1) with the Gaussian 09 (Revision E.01) suite of programs.[28] Although the nitro group has a negative effect on the $\Delta_f H^o$ of the corresponding energetic molecule, octanitro derivative **3** still exhibits the highest positive $\Delta_f H^o$ at 1.20 kJ g^{-1} which is attributed to the azo linkage and the large number of N-N or N=N bonds from the triazole rings. The $\Delta_f H^o$ values of fused triazolone derivatives **4**, **5**, and, **7**-**9** fall between -0.06 kJ g^{-1} and 1.04 kJ g^{-1}.

Using heats of formation and measured densities, energetic parameters were computed by using Explo5 v6.05 software.[29] Oxidizer **3** has excellent detonation properties (v_D, 8890 m s^{-1}, *P*, 33.9 Gpa), which are superior to those of AP (v_D, 6368 m s^{-1}; *P*, 15.8 GPa) and are comparable with those of HNF (v_D, 8948 m s^{-1}; *P*, 34.4 GPa) (Table 1). The detonation properties of the two potassium salts **4** (v_D, 8235 m s^{-1}, *P*, 29.7 Gpa) and **5** (v_D, 8756 m s^{-1}, *P*, 29.8 Gpa) exceed those of lead azide (33.4 GPa, 5877 m·s^{-1}). The neutral fused triazolone **7** has a superior detonation velocity of 9164 m s^{-1} and detonation pressure of 37.4 GPa. The ammonium salt of fused triazolone **8** (v_D, 8410 m s^{-1}, *P*, 29.2 Gpa) is less energetic than its *N*-oxide product **9** (v_D, 8727 m s^{-1}, *P*, 32.6 Gpa). The values of the impact and friction sensitivities were obtained by using a standard BAM drophammer apparatus and BAM friction tester, respectively. As indicated by the huge content of O···O interactions, the impact and friction sensitives of **3** are 5 J and 120 N, respectively, but which are less sensitive than those of ADN (IS, 3-5 J; FS, 64-72 N) and HNF (IS, 4 J; FS, 28 N). The potassium salts (**4**, 1 J, 60 N; **5**, 4 J, 144 N) are more sensitive than their ammonium salts (**8**, 4 J, 120 N; **9**, 10 J, 240 N). The presence of *N*-oxide in **5** and **9** is helpful in decreasing the sensitivities.

Oxygen balance (OB) is an important parameter to evaluate an energetic material since it stands for the completeness of the energy release of the energetic material after explosion. For an oxidizer, OB measures the supply ability of oxygen. The OB value of **3** is 29%, which is a little lower than AP (34%) and higher than those of ADN (26%), HNF (13%) and most trinitromethyl derivatives (Fig. 1b). Introduction of an *N*-oxide moiety is an effective way to enhance the OB of an energetic material. This is seen with the salts of fused triazolone *N*-oxide **5** (10%) and **9** (0%) having higher OB than their analogues **4** (7%) and **8** (-4%). The specific impulse (I_{sp}), another significant measure of the efficiency of a propellant (in seconds), was also calculated by using Explo. 5 v6.05 (Table 1). The oxidizer **3** has a specific impulse of 243 s, which is much higher than those of AP (157 s), and ADN (202 s). These properties suggest that **3** is an applicable and a very competitive highly dense oxidizer to replace AP in rocket propellants. The ammonium salts **8** (242 s) and **9** (253 s) have higher specific impulses than their potassium salts **4** (209 s) and **5** (219 s). It is found that the presence of *N*-oxide can also

Table 1. Properties of energetic compounds 3-5 and 7-9 compared with, ADN, HNF, AP and $Pb(N_3)_2$.

Comp.	T_d[a](°C)	ρ[b] (g cm^{-3})	$\Delta_f H°$[c] (kJ g^{-1})	v_D[d] (m s^{-1})	P[e] (GPa)	IS[f] (J)	FS[g] [N]	OB[h] (%)	I_{sp}[i] (s)
3	175	1.91	1.20	8890	33.9	5	120	29	253
4	277	2.07	-0.06	8235	29.7	1	60	7	209
5	292	2.13	0.05	8756	29.8	4	144	10	219
7	129	1.91	1.04	9164	37.4	8	180	12	261
8	175	1.78	0.60	8410	29.2	4	120	-4	242
9	202	1.83	0.70	8727	32.6	10	240	0	253
ADN	159	1.81	-1.13	7860	23.6	3-5	64-72	26	202
HNF	131	1.86	2.3	8948	34.4	4	28	13	265
AP	240	1.95	-2.52	6368	15.8	20	360	34	156
$Pb(N_3)_2$	315	4.800	1.55	5877	33.4	2.5-4	0.1-1	-11	-

[a] Decomposition temperature (onset) (5 °C min^{-1}). [b] Density measured by a gas pycnometer at room temperature. [c] Heat of formation. [d] Detonation pressure. [e] Detonation velocity. [f] Impact sensitivity. [g] Friction sensitivity. [h] Oxygen balance (based on CO) for $C_aH_bO_cN_d$, 1600(c-a-b/2)/M_W, M_W = molecular weight. [i] Specific impulse (calculated at an isobaric pressure of 70 bar and initial temperature of 3300 K. (The expansion conditions are equilibrium expansion). [j] kJ mol^{-1}. [k] Density from X-ray structural analysis. [l] kbar.

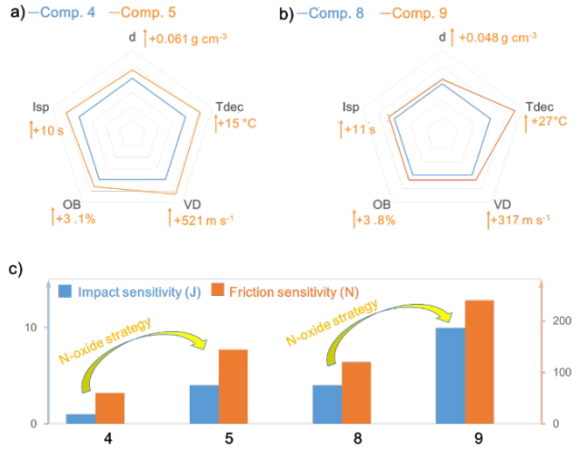

Fig. 5 Comparative properties of fused triazolones (**4** and **8**) and their *N*-oxides (**5** and **9**): (a) Radar chart of physicochemical properties for **4** and **5**. (b) Radar chart of physicochemical properties for **8** and **9**. (c) Clustered columns of mechanical sensitivity for **4**, **5**, **8** and **9**.

increase the specific impulse of the corresponding materials. The enhanced molecular stability and high performance indicate that FNTO salts could be potential alternative components of NTO salts in composite solid propellants. Furthermore, based on the overall parameters of sensitivity and energy, **5** shows the application potential as a lead azide replacement towards green primary explosive.

A comprehensive comparison was carried out based on thermal stability, density and detonation performance and mechanic sensitivity (Fig. 5). In terms of energetic ingredients, even 3-5% improvement of key parameters, e.g., density and detonation velocity, can significantly enhance the overall performance in the practical application (such as the replacement of RDX with HMX).[30,31] As can be seen in Fig. 5a and 5b, the energetic properties of *N*-oxide compounds **5** and **9** exhibit increases of 3% to 11% than those of **4** and **8**, respectively. More interestingly, the *N*-oxide strategy not only enhances the energy level and thermal stability, but also contributes greatly to modify the overall mechanical sensitivity (Table 1 and Fig. 5c). Functionalizing with *N*-oxide, the impact sensitivity (IS) and friction sensitivity (FS) of **5** are lower than those of **4** (**4**, IS, 1 J; FS, 60 N; **5**, IS, 4 J, FS, 144 N), and a similar trend can be found in comparative data of **8** and **9** (**8**, IS, 4 J; FS, 120 N; **9**, IS, 10 J, FS, 240 N). These comparisons highlight the *N*-oxide strategy as an effective functional modification to enhance thermal stability, I_{sp}, OB, and detonation properties, and decrease the sensitivities of an energetic material.

Conclusions

In summary, the azo functionality serves in the dual role of a bridge for the highly dense oxidizer **3** as well as a building block for construction of fused nitrotriazolones **4**, **5**, and **7**-**9**. While oxidizer **3** exhibits an excellent thermal stability and a high density compared with most polynitro compounds, FNTO derivatives **4** and **5** exhibit outstanding properties superior to

the analogous NTO salts, illustrating that an azo-based large π-conjugated system is conducive to high density and good thermal stability. 2D fingerprint plot and noncovalent interaction analysis of crystal **3** show that its dimeric stabilization is dominated by face-to-face π-π stacking interactions, which is enhances the density and stability of **3**. Compound **3** exhibits excellent physical performance (T_d, 175 °C, ρ, 1.91 g cm^{-3}, v_D, 8890 m s^{-1}, P, 33.9 Pa), has a high OB of 29%, and has a promising specific impulse (253 s), making it an applicable high energy dense oxidizer to replace AP in solid rocket propellants and missiles. Benefiting from both backbone and functionality, **5** has an excellent decomposition temperature of 292 °C and high energetic performance (v_D, 8756 m s^{-1}; P, 29.8 GPa), which may provide an alternative green solution for replacement of lead-based initiating substances. The molecular form of the fused triazolone, **7**, has a high density of 1.910 g cm^{-3} and excellent energetic properties that meet the requirements of advanced high explosives. It is worth noting that the azo bridge and *N*-oxide are effective strategies to pursuit excellent energetic materials with high thermal stability, density, detonation property, OB, I_{sp}, and low sensitivity. Additionally, the controllable reductive cyclization enriches the structural diversity of fused high-nitrogen heterocycles, thus expanding advanced synthetic strategies for future energetic materials.

Author Contributions

Qiong Yu and Fengsheng Li contributed equally.

Conflicts of interest

There are no conflicts to declare.

Acknowledgements

Financial support was received from the U.S. Office of Naval Research (N00014-16-1-2089), the Defense Threat Reduction Agency (HDTRA 1-15-1-0028), and National Natural Science Foundation of China (No. 22075023). The Rigaku Synergy S Diffractometer was purchased with support from the MRI program by the National Science Foundation Grant No. 1919565.

Notes and references

1 M. Benz, T. M. Klapötke, B. Krumm, M. Lommel and J. Stierstorfer, *J. Am. Chem. Soc.,* 2021, **143**, 1323-1327.
2 Y. Tang, W. Huang, G. H. Imler, D. A. Parrish and J. M. Shreeve, *J. Am. Chem. Soc.,* 2020, **142**, 7153-7160.
3 M. Deng, Y. Feng, W. Zhang, X. Qi and Q. Zhang, *Nat. Commun.*, 2019, **10**, 1339.
4 D. Trache, F. Maggi, I. Palmucci, L. T. DeLuca, K. Khimeche, M. Fassina, S. Dossi and G. Colombo, *Arabian J. Chem.,* 2019, **12**, 3639-3651.
5 C. W. Dennis and P. Sutton, *Joint Propulsion Conference & Exhibit*, Tucson, Arizona, 41th July 2005, 1-10.
6 M. Y. Nagamachi, J. I. S. Oliveira, A. M. Kawamoto and R. d. C. L. Dutra, *J. Aerosp. Technol. Manag.*, 2009, **1**, 153-160.
7 H. S. Jadhav, M. B. Talawar, D. D. Dhavale, S. N. Asthana and V. N. Krishnamurthy, *Indian J. Chem. Technol.*, 2005, **12**, 187-192.
8 Y. Zhou, H. Gao and J. M. Shreeve, *Energ. Mater. Front.,* 2020, **1**, 2-15.
9 M. A. Kettner and T. M. Klapötke, *Chem. Commun.,* 2014, **50**, 2268-2270.
10 M. Abd-Elghany, T. M. Klapötke and A. Elbeih, *Int. J. Energ. Mater. Chem. Propuls*., 2018, **17**, 349-357.
11 G. Zhao, P. Yin, D. Kumar, G. H. Imler, D. A. Parrish and J. M. Shreeve, *J. Am. Chem. Soc.*, 2019, **141**, 19581-19584.
12 V. Thottempudi, H. Gao and J. M. Shreeve, *J. Am. Chem. Soc.* 2011, **133**, 6464-6471.
13 Q. Ma, H. Gu, J. Huang, F. Nie, G. Fan, L. Liao and W. Yang, *New J. Chem.*, 2018, **42**, 2376-2380.
14 Q. Ma, G. Zhang, J. Li, L. Liao, J. Huang, G. Fan and F. Nie, *Chem.Select*, 2018, **3**, 1650-1654.
15 T. S. Hermann, T. M. Klapötke, B. Krumm and J. Stierstorfer, *New J. Chem.*, 2017, **41**, 3068-3072.
16 S. Dharavath, J. Zhang, G. H. Imler, D. A. Parrish and J. M. Shreeve, *J. Mater. Chem. A*, 2017, **5**, 4785-4790.
17 V. V. Semenov, S. A. Shevelev, A. B. Bruskin, A. K. Shakhnes and V. S. Kuz'min, *Chem. Heterocycl. Compd.*, 2017, **53**, 728-732.
18 G. Singh and S. Prem Felix, *Combust. Flame*, 2003, **135**, 145-150.
19 T. Liu, X. Qi, K. Wang, J. Zhang, W. Zhang and Q. Zhang, *New J. Chem.*, 2017, **41**, 9070-9076.
20 Y. Li, N. Liu, P. Su, Y. Wang, Z. Ge, H. Li and B. Wang, *Asian J. Chem.*, 2014, **26**, 7151-7156.
21 T. P. Kofman, A. E. Trubitsin, I. V. Dmitrienko and E. Y. Glazkova, *Russ. J. Org. Chem.* 2008, **44**, 874-881.
22 A. V. Parwani and D. Jayatilaka, *CrystEngComm*, 2009, **11**, 19-32.
23 B. Tian, Y. Xiong, L. Chen and C. Zhang, *CrystEngComm*, 2018, **20**, 837-848.
24 E. R. Johnson, S. Keinan, P. Mori-Sanchez, J. Contreras-Garcia, A. J. Cohen and W. Yang, *J. Am. Chem. Soc*., 2010, **132**, 6498-6506.
25 F. Neese, *WIREs Comput. Mol. Sci*., 2012, **2**, 73-78.
26 T. Lu and F. Chen, *J. Comput. Chem.*, 2012, **33**, 580-592.
27 W. Humphrey, A. Dalke and K. Schulten, *J. Mol. Graph. Model*., 1996, **14**, 33-38.
28 M. J. Frisch, G. W. Trucks, H. B. Schlegel, G. E. Scuseria, M. A. Robb, J. R. Cheeseman, G. Scalmani, V. Barone, B. Mennucci, G. A. Petersson, H. Nakatsuji, M. Caricato, X. Li, H. P. Hratchian, A. F. Izmaylov, J. Bloino, G. Zheng, J. L. Sonnenberg, M. Hada, M. Ehara, K. Toyota, R. Fukuda, J. Hasegawa, M. Ishida, T. Nakajima, Y. Honda, O. Kitao, H. Nakai, T. Vreven, J. A. Montgomery, Jr., J. E. Peralta, F. Ogliaro, M. Bearpark, J. J. Heyd, E. Brothers, K. N. Kudin, V. N. Staroverov, T. Keith, R. Kobayashi, J. Normand, K. Raghavachari, A. Rendell, J. C. Burant, S. S. Iyengar, J. Tomasi, M. Cossi, N. Rega, J. M. Millam, M. Klene, J. E. Knox, J. B. Cross, V. Bakken, C. Adamo, J. Jaramillo, R. Gomperts, R. E. Stratmann, O. Yazyev, A. J. Austin, R. Cammi, C. Pomelli, J. W. Ochterski, R. L. Martin, K. Morokuma, V. G. Zakrzewski, G. A. Voth, P. Salvador, J. J. Dannenberg, S. Dapprich, A. D. Daniels, O. Farkas, J. B. Foresman, J. V. Ortiz, J. Cioslowski and D. J. Fox, Gaussian 09, Revision B.01, Gaussian, Inc., Wallingford CT, 2010.
29 EXPLO5 (Version 6.05), M. Suceska, OZM Research s. r. o, Pardubice, 2018.
30 A. A. Dippold and T. M. Klapötke, *J. Am. Chem. Soc.*, 2013, **135**, 9931-9938.
31 D. E. Chavez, D. A. Parrish, L. Mitchell and G. H. Imler, *Angew. Chem. Int. Ed.*, 2017, **56**, 3575-3578.

